

IMPLICATIONS OF STOKES–CARTAN THEOREM TO TIME-HARMONIC ACOUSTIC BOUNDARY INTEGRAL EQUATION FORMULATIONS

PAUL J. SCHAFBUCH*

Iowa State University, Mechanical Engineering Department and Center for Nondestructive Evaluation, USA

ABSTRACT

Direct boundary integral equation (BIE) formalisms for wave radiation and scattering have been stable and universally accepted for decades. Yet, the classic separation of variables (SOV) solutions for acoustic radiation and scattering from spheres do not always agree with BEM results. For certain conditions, the boundary acoustic field predicted by low-frequency SOV and BEM methods match exactly and for other situations predicted fields by the two methods are complex-conjugates of each other. While this difference is subtle, modern BEM literature has not cited the transfer of known mathematics to this engineering application. Tracing signs within BEM code is daunting. To create a lucid and reproducible record of the issue and its resolution, this paper presents an analytical BIE solution for spherical geometry based on a Legendre polynomial simplex element and a power series of the spatial phase term of the Helmholtz operator Fundamental Solution. Optical theorem reasoning suggests the traditional BIE approach is the method in error. The core of this issue is the application of the divergence theorem (strictly true only for real-valued functions) to time-harmonic (complex-valued) formulations. The conjugation of spatial derivatives of a complex-valued field can be understood from Wirtinger derivatives and Dolbeault operators. This issue manifests itself when the Sommerfeld radiation condition is applied for unbounded domains. Exterior calculus ideas properly unite, generalize and extend a variety of related classical theorems including divergence, Cauchy's integral theorem from complex analysis, and Green's identities used in constructing a BIE. The resulting Stokes–Cartan theorem is properly applied to acoustic scattering in 3D within this paper and invokes corrections which match BIE and SOV solutions for the low frequency problems investigated.

Keywords: boundary integral equation, time-harmonic, acoustic, scattering, Kirchhoff–Helmholtz integral, Wirtinger derivative, optical theorem.

1 INTRODUCTION

Boundary integral equation methods are inherently well-suited for simulating exterior domain wave phenomena, in both time and time-harmonic formulations. Wave scattering boundary value problems (BVP) are often idealized with a “boundary” at infinite distance even though the corresponding physical arrangement has limited dimensions. In applications such as nondestructive testing, the illuminating wave may be a pulse or tone burst, and substantial complication of echoes from all the boundaries of the continuum is avoided by time gating the experimental scattered waves prior to the arrival of any unwanted reflected waves. Consequently, the infinite boundary treatment of the BIE approach is ideal. The only caveat is to invoke the well-established Sommerfeld radiation condition to preclude any inbound waves coming from infinity. Due to the computational advantages (in many cases) over time-marching schemes, frequency domain formulations are quite popular and the function describing the spatial distribution of the waves is (of course) *complex-valued*.

A combination of circumstances specific to this class of problems is believed to create a more complicated mathematical situation than has been widely discussed within the BEM community. The calculus pillar on which BIE methods rest is the divergence theorem (or you

* ORCID: <http://orcid.org/0000-0002-9256-7893>



may say, the related and specifically tailored Green's third identity). It is hardly a secret that the divergence theorem is only proven for *real-valued* functions. Katz [1] provides perspective of the evolution of the Stokes theorem family from the time of Gauss, through Green, and up to Élie Cartan. It was Cartan who in 1945 published the modern generalizations of Stokes' theorem (GST) which included complex-valued functions on a complex-valued manifold [2]. The GST is part of 20th century *Exterior Calculus*.

These extensions to calculus do not automatically imply that there are any modification to our class of problems needed. Indeed, BIE methods for exterior domain wave phenomena seem amply verified against other methods decades ago. This author produced confirmations of elastic wave scattering amplitude *magnitudes* with Schafbuch et al. against SOV and method of optimal truncation years ago [3], [4]. In some cases, benchmark information included real and imaginary components and our BEM was producing (rather precisely) the complex conjugate. The presumed cause was a programming error – which was never found, and dismissed as such, at the time. After a career elsewhere, this issue is being revisited. Astonishingly, I have found a conjugated result in simple acoustic radiation benchmarks.

The author admits how outlandish these claims are. The secondary objective of this paper is to create a discussion of what is known or has been experienced on this subject in the BIE/BEM community, which was not, or at least is no longer mentioned. Section 5 contains a review of rather old mathematics on this topic, and suggests a rethinking of the implications of the Cartan generalization. But first, we present the primary objective – an analytical BIE which can be verified and/or recreated without the ambiguity of debugging BEM code.

We infer this issue is systemic to all wave phenomena if analysed by direct time-harmonic BIE applied to unbounded exterior domains in *three* dimensions. The scalar nature of acoustic waves provides the least complicated model to explore this issue. Kirkup [5] provides a recent and extensive review of BEM technology applied to acoustics. This author was unable to locate any discussion of the current paper's noted concern in any of Kirkup's exhaustive and up-to-date reference list. Kirkup's excellent discussion also does not raise this issue with time-harmonic formulations. He does state the standard BIE for wave scattering which is likewise our starting point for analytically implementing the traditional approach. The direct acoustic pressure field (P) is governed by:

$$\frac{1}{2}P = \int_S \left\{ G \frac{\partial P}{\partial n} - P \frac{\partial G}{\partial n} \right\} d\xi + {}^I P. \quad (1)$$

For simplicity and to take advantage of available long-standing SOV solutions we restrict our investigation to a spherical boundary – parameterized by standard spherical coordinates $\langle r, \theta, \phi \rangle$ with radius (a).

$$\frac{1}{2}P = \int_0^\pi \int_0^{2\pi} \left\{ G \frac{\partial P}{\partial n} - P \frac{\partial G}{\partial n} \right\} a \sin \theta d\phi a d\theta + {}^I P. \quad (2)$$

A brief note about nomenclature: upper case Latin and Greek characters are complex-valued quantities, and lower case are real-valued, except for i itself. Single character pre-superscripts denote a type of field quantity such as (I)ncident, (S)cattered, or (T)otal. Pre-subscripts denote a specific location. Trailing subscripts are reserved for direction indices of future vector/tensor formulations. For scalar quantities, this post-subscript can be a series index. Tilda accents (\sim) mean approximate and grave ($\grave{}$) indicates time dependence is explicit.



2 ANALYTICAL AXISYMMETRIC LONG WAVELENGTH APPROXIMATION

In order to obtain a traceable closed form solution with minimal algebraic complications (i.e., chance for error) we also restrict our analysis to axisymmetric boundary conditions and/or incident field. The direction of propagation of a plane wave incident field, then defines the axis of symmetry, as shown in Fig. 1(a). The axial symmetry makes the (ϕ) integration trivial. We also convert to Lagrange notation for the (normal) spatial derivative.

$$P = 4\pi \int_0^\pi \{GP' - PG'\} a \sin \theta \, d\theta + 2 {}^L P. \quad (3)$$

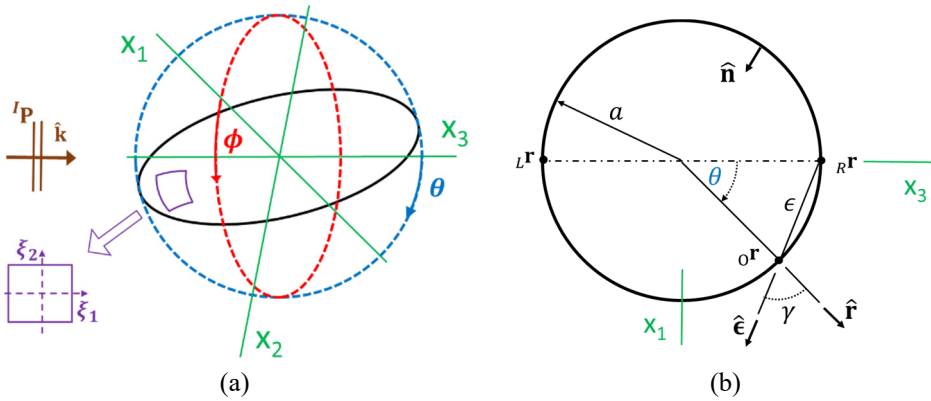


Figure 1: Boundary surface and incident wave geometric definitions. (a) Spherical coordinates polar angle (θ) measured from positive Cartesian coordinate (X_3) with incident plane wave propagating in the X_3 direction. Surface patch in terms of coordinates $\{\theta, \phi\}$ is conceptually mapped to unit square with $\{\xi_1, \xi_2\}$ coordinates; and (b) Planar view of axisymmetric geometry at $\{\phi = 0\}$ with (L)eft and (R)ight nodal positions (r) defined on the polar axis. Fundamental solution cord length (ϵ) and propagation direction (\hat{e}) are shown, as well as outward surface normal (\hat{n}) and radial (\hat{r}) unit vectors.

2.1 A most simple discretization for a sphere's surface

A long wavelength assumption allows the surface acoustic field to be interpolated linearly along global coordinate (x_3) . The entire sphere surface is interpolated by a single axisymmetric simplex element with nodal values $({}^L P)$ and $({}^R P)$. The axial position (x_3) is expressed in terms of polar angle (θ) . This element reproduces the first two Legendre polynomials – utilized by standard SOV solutions of this problem

$$P(\theta) \cong {}^L P \frac{1}{2} \left[1 - \frac{(a \cos \theta)}{a} \right] + {}^R P \frac{1}{2} \left[1 + \frac{(a \cos \theta)}{a} \right]. \quad (4)$$

Both the surface field and its normal derivative are estimated by a constant and a linear term. The node-value based form for the normal derivative is illustrated:

$$P'(\theta) \cong \frac{1}{2} \left[{}^L P' + {}^R P' \right] + \frac{1}{2} \left[{}^R P' - {}^L P' \right] \cos \theta. \quad (5)$$

We can define some surface integrals which appear repeatedly for various boundary conditions of radiation and scattering BVPs. For the constant term,

$${}_0V = 2\pi \int_0^\pi \{G\} a \sin \theta a \, d\theta, \quad {}_0W = -2\pi \int_0^\pi \{G'\} a \sin \theta a \, d\theta. \quad (6)$$

For the linear term,

$${}_1V = 2\pi \int_0^\pi \{G\} a \sin \theta \cos \theta a \, d\theta, \quad {}_1W = -2\pi \int_0^\pi \{G'\} a \sin \theta \cos \theta a \, d\theta. \quad (7)$$

2.2 Acoustic fundamental solutions for exterior domains

For an exterior domain radiation BVP, the outgoing wave fundamental solution is of interest. For the Helmholtz operator in 3D, this Green's function is well known

$${}^s\hat{G} = \frac{-\exp(+ik\epsilon - i\omega t)}{4\pi\epsilon} \quad \text{with} \quad \epsilon = \|\mathbf{x} - \mathbf{o}\|. \quad (8)$$

We utilize the symbol (ϵ) for the distance between generic field point \mathbf{r} with vector Cartesian coordinate (\mathbf{x}) and the boundary source point \mathbf{o} (for origio, as in *fons et origio*). This form of the fundamental solution explicitly shows the time dependence, clarifying the outgoing wave nature. In upcoming notation (sG) the time dependence is suppressed, as is traditionally done. The complete Fundamental Solution also includes the companion *incoming wave* Green's function (pG). (G) denotes the union of both potential solution forms. Note for future reference that this solution pair are complex conjugates, i.e., ${}^sG = {}^pG^\dagger$. The well accepted Sommerfeld radiation condition precludes consideration of non-physical incoming waves from the boundary at infinity.

2.2.1 Spatial derivative of fundamental solution in the normal direction

We construct the normal derivative of G from the gradient, utilizing Fig. 1(b), and noting that the only spatial variation is in the direction of ($\hat{\mathbf{e}}$). The cord length (ϵ) from point \mathbf{o} to point \mathbf{r} is simply $\{2a \sin(\theta/2)\}$. Also from this figure, $\{\gamma = (\pi - \theta)/2\}$, therefore $\{\cos \gamma = \sin(\theta/2) = \epsilon/2a\}$. Hence the normal derivative is:

$${}^sG' = \frac{\partial G}{\partial n} = \hat{\mathbf{n}} \cdot \nabla {}^sG = -\cos \gamma \frac{\partial {}^sG}{\partial \epsilon} = -\frac{\epsilon}{2a} \frac{\exp(ik\epsilon)}{4\pi\epsilon^2} [1 - ik\epsilon]. \quad (9)$$

2.2.2 Low frequency approximation of the fundamental solution

The spatially oscillating complex exponential in the fundamental solution and its derivative, is approximated as a fourth order power series of ($k\epsilon$) in the linear terms:

$$\exp(ik\epsilon) \cong [1 - (k\epsilon)^2/2 + (k\epsilon)^4/24] + i[k\epsilon - (k\epsilon)^3/6]. \quad (10)$$

2.3 Evaluation of the surface integrals

The integrals of eqn (6) can be evaluated exactly using a double angle trigonometry identity and realizing $\{a \sin \theta a \, d\theta = \epsilon \, d\epsilon\}$.

$${}_0V = -\frac{1}{2} \int_0^{2a} \exp(ik\epsilon) d\epsilon = \frac{i}{2k} [\exp(i2ka) - 1]. \quad (11)$$

The integral of the gradient of the Green's function uses the findings of eqn (9), integral tables, and some post integration algebraic manipulation to simplify to:



$${}_0W = \frac{1}{4a} \int_0^{2a} \{ \exp(ik\epsilon) [1 - ik\epsilon] \} d\epsilon = [1 - \exp(i2ka)] \frac{ka-i}{2ka} - \frac{1}{2}. \quad (12)$$

The integrals of eqn (7) require use of the power series of eqn (10). Introduce temporary abbreviations $\{ \mathfrak{s} = \sin(\theta/2) \}$ and $\{ \mathfrak{c} = \cos(\theta/2) \}$. Again using $\{ \epsilon = 2a\mathfrak{s} \}$, and now the half-angle trigonometric identity for $\cos \theta$, the approximated value for ${}_1V$ is:

$${}_1\tilde{V} = a/2 \int_0^\pi \left\{ \left[1 - \frac{4}{2}(ka)^2 \mathfrak{s}^2 + \frac{16}{24}(ka)^4 \mathfrak{s}^4 \right] + i \left[2ka\mathfrak{s} - \frac{8}{6}(ka)^3 \mathfrak{s}^3 \right] \right\} [\mathfrak{s}^2 \mathfrak{c} - \mathfrak{c}^3] d\theta. \quad (13)$$

Then defining a trigonometric definite integral family:

$$\zeta_{mq} = \int_0^\pi \left[\left(\sin \frac{\theta}{2} \right)^m \left(\cos \frac{\theta}{2} \right)^q \right] d\theta = \int_0^\pi [\mathfrak{s}^m \mathfrak{c}^q] d\theta. \quad (14)$$

Exact values for (ζ) utilized in these truncated power series expansions are: $\{ \zeta_{21} = 2/3 \}$, $\{ \zeta_{31} = 1/2 \}$, $\{ \zeta_{41} = 2/5 \}$, $\{ \zeta_{51} = 1/3 \}$, $\{ \zeta_{61} = 2/7 \}$, $\{ \zeta_{03} = 4/3 \}$, $\{ \zeta_{13} = 1/2 \}$, $\{ \zeta_{23} = 4/15 \}$, $\{ \zeta_{33} = 1/6 \}$, and $\{ \zeta_{43} = 4/35 \}$.

Our surface integral then reduces to a sum of powers of dimensionless frequency (ka) ,

$${}_1\tilde{V} = -a \left\{ \left[\frac{1}{3} + \frac{2}{15}(ka)^2 - \frac{2}{35}(ka)^4 \right] + i \left[\frac{1}{9}(ka)^3 \right] \right\}. \quad (15)$$

An analogous procedure is used to evaluate the surface integral involving the Green's function derivative for the linear BEM interpolation. Only algebraic details differ, so we offer the result directly. Some readers may wonder why no explicit regularization or Cauchy Principal Value interpretation was mentioned. Recall we have an ideally smooth surface element where the BEM Jacobian is zero as $\{ \epsilon \rightarrow 0 \}$ in the normal gradient integral

$${}_1\tilde{W} = \frac{1}{2} \left\{ \left[\frac{1}{3} - \frac{2}{15}(ka)^2 + \frac{6}{35}(ka)^4 \right] - i \left[\frac{2}{9}(ka)^3 \right] \right\}. \quad (16)$$

2.4 Approximation for a plane wave incident field

The expression for incident wave acoustic pressure (${}^I P$) in a time-harmonic formulation has been approximated to exceed the axial linear-in-space interpolation of the long wavelength BEM, to provide better accuracy. It is represented in powers of (ka) to be algebraically combined with the preceding surface integrals. Propagation is in the $(+x_3)$ direction. For simplicity, the wave amplitude is unity

$${}^I P = \exp(ikx_3) \cong {}^I \tilde{P} = [1 - (kx_3)^2/2] + i[kx_3 - (kx_3)^3/6]. \quad (17)$$

A valid argument can be made to include terms up to $(ka)^4$, although the spatial interpolation is more likely the limitation to accuracy.

3 ANALYTICAL BIE VERSUS SOV RESULTS FOR RADIATION BVP

Exterior domain radiation from a sphere has both time-domain analytical and SOV series solutions to validate the low-frequency BIE results. First, specialize eqn (3) to no incident field and utilize the nodal interpolation of eqn (5) and our expressions of the surface integrals

$${}_R P + {}_0 W [{}_L P + {}_R P] + {}_1 \tilde{W} [{}_R P - {}_L P] \cong {}_0 V [{}_L P' + {}_R P'] + {}_1 \tilde{V} [{}_R P' - {}_L P']. \quad (18)$$

In this “model” BIE, a force momentum considerations establish the relation between the spatial gradient of the pressure field and the radial fluid velocity (${}^R U$) based on density (ρ) and speed of sound (c)

$${}_R P' = ik\rho c({}_R U). \quad (19)$$

3.1 A pulsing (monopole-like) sphere

In this spherically symmetric case, eqn (18) greatly simplifies, since $\{ {}_L P = {}_R P \}$

$${}_R P + {}_0 W[2 {}_R P] = {}_0 V[2 {}_R P']. \quad (20)$$

Using eqns (11), (12) and (19), a relationship between the radial velocity and the pressure – both at the sphere surface. The pressure at the right node is the pressure everywhere on the sphere,

$${}_R P = \frac{ikapc}{1+ika}({}_{r=a} {}_R U). \quad (21)$$

Solutions to this type of problem date back to the 19th century, but Pierce [6] is a more accessible reference (among others) to validate this result. Eqn (21) seems familiar, but is exactly the complex conjugate of Pierce's equation (4-1.4) for the same benchmark case. The Pierce solution evolves from the time-domain wave equation as is detailed in his chapter 1.

In the next section, an SOV method as documented by Morse [7], is utilized for a second benchmark problem. That methodology has been used by this author to replicate the Pierce result. This exercise was intended to cross-validate those two methods, and reduce the likelihood of a sign convention issue, being the sole cause of the conjugated result of the BIE method. Nevertheless these results clearly suggest the analysis of Section 2 contains an error.

3.2 An axially oscillating (dipole-like) sphere

Another simple case with an analytical solution for long wavelengths is a rigid surface sphere moving harmonically along the axis of symmetry (L–R axis in Fig. 1(b)). For a finite size sphere, the radiated pressure in the far field approaches that of a theoretical dipole source. But to better evaluate our BIE paradox, we need the full richness of the SOV solution as detailed in Morse [7] and more fully explored by Morse and Ingard [8] at the sphere surface. M&I details an explicit far pressure field result, but we must utilize their methodology to characterise the induced surface pressure. An outline of steps taken is provided here to enable the reader to reproduce the result. The general time-harmonic SOV solution for sphere radiation and scattering utilizes spherical harmonics and 1st and 2nd kind spherical Bessel functions $\{j, \eta\}$ (for the radial direction). The axisymmetric distributions with polar angle are based on the orthogonal set of Legendre polynomials (\mathcal{P}_m). M&I equation (7.2.14) in the nomenclature of this paper is

$${}_R \dot{P}(r, \theta) = \sum_{m=0}^{\infty} A_m \mathcal{P}_m(\cos \theta) [j_m(kr) + i\eta_m(kr)] \exp(-i\omega t). \quad (22)$$

For this motion, a) the surface velocities on the left and right sides of the sphere are 180° out of phase; b) there is no phase variation within a given side; and c) the temporal basis is identical with the BIE basis (and will likewise be suppressed in upcoming equations). Consequently, the \mathcal{P}_1 function completely and exactly characterizes the surface normal velocity distribution – so only one term of the series is needed. M&I equation (7.2.15) allows the evaluation of A_1 . Then for unit amplitude rigid motion, the pressure at the right node,

$${}_R P = \frac{1}{2} \rho c (ka)^3 \exp(i(ka)^3/6) [j_1(ka) + i\eta_1(ka)]. \quad (23)$$

In order to compare with the upcoming BEM result, the exponential and spherical Bessel functions need to be expressed as truncated power series, such as

$$j_1(ka) \cong \frac{1}{3}(ka) - \frac{1}{30}(ka)^3. \quad \eta_1(ka) \cong \frac{-1}{(ka)^2} \left[1 + \frac{1}{2}(ka)^2 - \frac{1}{8}(ka)^4 \right]. \quad (24)$$

Truncating the product of all three series to fourth order in (ka) ,

$${}_R\tilde{P} = \rho c \left\{ \frac{1}{4}(ka)^4 - i \left[\frac{1}{2}ka + \frac{1}{4}(ka)^3 \right] \right\}. \quad (25)$$

Now to adapt discretized BIE eqn (18) to the case of an oscillating rigid sphere. The two sides' phase relationship causes $\{ {}_L P = -{}_R P \}$. While nodal velocities are identical, the surface normal direction at nodes L and R are reversed – yielding a similar cancellation of the zero order pressure gradient term. Also incorporating eqn (19) with unit amplitude motion yields:

$${}_R P + 2 {}_1\tilde{W} [{}_R P] \cong 2 {}_1\tilde{V} [ik\rho c]. \quad (26)$$

Using the surface integral formulae of eqns (15) and (16), creates an expression for the surface pressure at the right node for this second radiation benchmark case

$${}_R\tilde{P} = k\rho c \frac{\left\{ \left[\frac{1}{9}(ka)^3 \right] - i \left[\frac{1}{3} + \frac{2}{15}(ka)^2 - \frac{2}{35}(ka)^4 \right] \right\}}{\left\{ \left[\frac{2}{3} - \frac{1}{15}(ka)^2 + \frac{3}{35}(ka)^4 \right] - i \left[\frac{1}{9}(ka)^3 \right] \right\}}. \quad (27)$$

Algebraic manipulation of this expression with truncation of terms above fourth order in (ka) yields a simple polynomial in powers of (ka) that is identical to the SOV result of eqn (25).

This result deepens the dilemma of the conjugated results of the pulsing sphere case. The methodology needed for this dipole-like source including truncated power series, division of complex valued polynomials, trigonometric manipulation and integration is far more convoluted and error prone. Yet terms match to fourth order. One conclusion is that the error is isolated only to the zero order integrals ${}_0V$ and ${}_0W$ as these integrals were not used in the dipole radiation case. We move on to a rigid sphere scattering benchmark case, which utilizes ${}_0W$ and ${}_1\tilde{W}$ surface integrals. We will need the power series approximation of ${}_0W$ in order to combine terms symbolically. It was found that a direct conversion of the form which exactly cancels terms in ${}_0V$ is an awkward approximation. The process used for of ${}_1W$ with the sine and cosine integrals was utilized instead

$${}_0\tilde{W} = \left\{ \left[\frac{1}{2} + \frac{1}{3}(ka)^2 \right] + i \left[\frac{1}{3}(ka)^3 \right] \right\}. \quad (28)$$

4 ANALYTICAL BIE VERSUS SOV RESULTS FOR SCATTERING

The case of acoustic scattering from an immovable rigid spherical surface has been the reference problem for scattering theory for decades. Chapter 8 of Morse and Ingard [8] is a seminal reference and is utilized here. The boundary condition in our pressure formulation is homogeneous Neumann. Beginning with the more general eqn (3), we create a discretized version for the scattering problem with this boundary condition;

$${}_R P + {}_0W [{}_L P + {}_R P] + {}_1\tilde{W} [{}_R P - {}_L P] \cong 2 {}_R^I P. \quad (29)$$

Due to the left–right asymmetry of the incident wave, the left and right nodal values of pressure are unique. We need a second equation for the other unknown value, and utilize the simple historical approach of also collocating the BIE at the left node. Recall the traditional

BIE for scattering problems is in terms of the TOTAL pressure (scattered plus incident). For clarity, the explicit pre-superscript “ ” has been added. Then in matrix form:

$$\begin{bmatrix} 1 + {}_0\tilde{W} + {}_1\tilde{W} & {}_0\tilde{W} - {}_1\tilde{W} \\ {}_0\tilde{W} - {}_1\tilde{W} & 1 + {}_0\tilde{W} + {}_1\tilde{W} \end{bmatrix} \begin{Bmatrix} {}^T_L P \\ {}^T_R P \end{Bmatrix} \cong 2 \begin{Bmatrix} {}^I_L \tilde{P} \\ {}^I_R \tilde{P} \end{Bmatrix}. \quad (30)$$

Combining all terms and showing the detail up to $(ka)^3$

$$\begin{bmatrix} \frac{5}{3} + \frac{4(ka)^2}{15} + i\frac{2}{9}(ka)^3 & \frac{1}{3} + \frac{2(ka)^2}{5} + i\frac{4}{9}(ka)^3 \\ \frac{1}{3} + \frac{2(ka)^2}{5} + i\frac{4}{9}(ka)^3 & \frac{5}{3} + \frac{4(ka)^2}{15} + i\frac{2}{9}(ka)^3 \end{bmatrix} \begin{Bmatrix} {}^T_L P \\ {}^T_R P \end{Bmatrix} \cong 2 \begin{Bmatrix} 1 - \frac{(ka)^2}{2} - ika + i\frac{(ka)^3}{6} \\ 1 - \frac{(ka)^2}{2} + ika - i\frac{(ka)^3}{6} \end{Bmatrix}. \quad (31)$$

This matrix can be analytically inverted by Cramer's rule. Back solving for the total pressure at the left node and truncating to third order:

$${}^T_L P \cong \left\{ \left[1 - \frac{5}{6}(ka)^2 \right] - i \left[\frac{3}{2}ka + \frac{7}{30}(ka)^3 \right] \right\}. \quad (32)$$

4.1 Traditional SOV approximate solution

The method in section 8.2 of M&I [8] produces a direct estimate for the scattered pressure distribution at the rigid sphere surface. The Legendre series solution was truncated after two terms, which provides accuracy on the order of $(ka)^3$. Unlike the two radiation cases, other terms are not identically zero – due to the left–right asymmetry of the incident pressure field and a phase variation in the response along the L–R axis. Since the BEM simplex element and the two-term SOV spatial interpolations are identical, comparing the power series at a single location is representative of all points. The comparison is at the left node location. The incident pressure terms (shown in the top entry of the RHS vector of eqn (31) are added to the scattered pressure for a direct comparison with eqn (32). There is some difference in the $(ka)^3$ term due to truncation, but no conjugation and no other significant differences. Equation (9-1.8) of Pierce [6] produces an identical result to eqn (33).

$${}^T_L P \cong \left\{ \left[1 - \frac{5}{6}(ka)^2 \right] - i \left[\frac{3}{2}ka + \frac{5}{12}(ka)^3 \right] \right\}. \quad (33)$$

5 A RADIATION BIE BASED ON EXTERIOR CALCULUS

The generalization of Stokes' theorem is normally expressed in the language of *differential forms*. This calculus of the 20th century is both fully compatible with classical vector calculus and uses similar symbolism, but with highly abstracted meaning. Fortunately, our purpose only requires basic ideas, many easily self-teachable from Fortney [9] and Nakahara [10]. To be clear, this paper absolutely does not introduce any new mathematical ideas.

5.1 Useful elementary ideas of exterior calculus of complex-valued forms

We begin with the Stokes–Cartan theorem itself relating a generic complex function (Ξ) defined in a volumetric domain (\mathcal{C}) to its boundary (\mathcal{S}):

$$\int_{\mathcal{C}} d\Xi = \int_{\mathcal{S}} \Xi; \quad \text{and in our acoustic BIE case, } \Xi = GP' - PG'. \quad (34)$$

While eqn (34) is a much more general statement, we will only consider a 3D domain with “2D” boundary constructible from a series of patches as shown in Fig. 1(a). This statement also shows a characteristic of *differential forms*, where the variables of integration are not shown. A central tenant is that the value of an integral is invariant to the choice of

independent variables mapping its domain, an idea we shall use. Eqn (34) states that the volume integral of the exterior derivative operator (d) on a 0-form (i.e., a function) is equivalent to the integral of that 0-form over the domain's oriented boundary. Ξ can be a vector function so this approach is extendable to electromagnetic and elastic wave phenomena. Here only the scalar (acoustic) case is considered. The basic theory requires a smooth boundary with a metric (*manifold*), the exterior derivative is then defined from rates of change (analogous to gradient operator) on the manifold's *tangent space* (a plane for a 3D domain).

Mapping is another key tenant of differential forms. Fig. 1(a) shows a map of a patch (element) of the manifold (comprised of q patches) to a rectilinear projection in terms of coordinates $\{\xi_1, \xi_2\}$. Eqn (34) can then be specialized to our 3D/2D case and recast to familiar vector calculus symbols but with explicit exterior derivatives of the mapped surface coordinates. Finally the map of the patch could be considered to be on the complex plane with a single coordinate $\{Z \in \mathbb{C}\}$

$$\iiint_c d\Xi = \sum_q \oint_{\mathcal{S}} \Xi (d\xi_1 \wedge d\xi_2) = \sum_q \oint_{\mathcal{S}} \Xi dZ. \quad (35)$$

This equation utilizes the exterior product symbol (\wedge). Also known as a wedge product, the rules of exterior algebra define $\mathbf{h} \wedge \mathbf{b} = \mathbf{h} \otimes \mathbf{b} - \mathbf{b} \otimes \mathbf{h}$ with (\mathbf{h}) and (\mathbf{b}) being column vectors. Further, the outer product is defined as $\mathbf{h} \otimes \mathbf{b} = \mathbf{h}\mathbf{b}^T$, making the result a *bivector*. The common *cross product* of vector calculus (in 3D) creates a pseudo-vector analogous to the wedge product's bivector. Thus the mechanisms of exterior algebra automatically create the boundary surface normal derivative vector which appears in the divergence theorem. The manifold's normal derivative can be determined from differentiation in the complex plane.

5.1.1 Wirtinger derivatives

In the segue from Riemann to the results of Cartan [2], Wirtinger introduced formalisms for the differentiation of a complex valued function of a complex variable [11]. Using the standard variables for the real and imaginary parts $\{Z = x + iy\}$ and the overbar ($\bar{}$) denoting conjugation, the exterior derivative can be split into two parts $\{\partial + \bar{\partial}\}$ known as Dolbeault operators, that were anticipated by Wirtinger as:

$$\partial = \frac{\partial}{\partial z} = \frac{1}{2} \left(\frac{\partial}{\partial x} - i \frac{\partial}{\partial y} \right), \quad \bar{\partial} = \frac{\partial}{\partial \bar{z}} = \frac{1}{2} \left(\frac{\partial}{\partial x} + i \frac{\partial}{\partial y} \right). \quad (36)$$

If the function (H) these operators are acting on is holomorphic, that function solves the Cauchy–Reimann equations and $\{\bar{\partial}H \equiv 0\}$. If we apply the remaining Wirtinger derivative to our fundamental solutions, we need to use a slightly more complicated complex-analysis chain rule and an associated conjugate differentiation rule. They are generically:

$$\frac{\partial}{\partial z} (\Theta \circ E) = \left(\frac{\partial \Theta}{\partial z} \circ E \right) \frac{\partial E}{\partial z} + \left(\frac{\partial \Theta}{\partial \bar{z}} \circ E \right) \frac{\partial \bar{E}}{\partial z}; \quad \text{and} \quad \overline{\left(\frac{\partial \Theta}{\partial z} \right)} = \frac{\partial \bar{\Theta}}{\partial \bar{z}}. \quad (37)$$

To apply this formalism to the Fundamental Solutions, composition is needed and distance (ϵ) appears twice. However, distance is always positive and real-valued which allows key simplifications. Still, after nontrivial manipulation, we reach the twin conclusions:

$$\partial [{}^s G] = \left[\frac{\partial}{\partial n} ({}^s G) \right]^\dagger; \quad \text{and} \quad \partial [{}^p G] = \left[\frac{\partial}{\partial n} ({}^p G) \right]^\dagger. \quad (38)$$

This result implies a spatial derivative in the normal direction from the rules of the divergence theorem is the conjugate of the appropriate application of exterior calculus. We will return to



the special case when $\{\epsilon \rightarrow 0\}$ in Section 5.2. Eqn (1) also contains a normal derivative of the complex-valued pressure field. With less complication, the anticipated conclusion is:

$$\partial[P] = \left[\frac{\partial}{\partial n}(P) \right]^{\dagger}. \quad (39)$$

5.1.2 Is the traditional radiation BIE truly a function of a complex variable?

In Cheng and Cheng [12], the long evolution of BEM is eloquently documented. During the 1960s, the promise of the method began to be pragmatically realized into elastostatics and time-harmonic acoustic calculations. Since 1971, Burton and Miller [13] is likely the most cited reference regarding the fictitious eigen-frequency issue and its theoretical resolution – which occurs in exterior domain wave phenomena simulations by BEM. Their paper progresses from Laplace’s to Helmholtz’s equation with no expressed concern of a complex-valued field. Likewise Colton and Kress [14] exhaustively consider BIE methods for wave scattering in a mathematically rigorous fashion, and even mention sesquilinear forms in chapter 1 – but do not mention a conjugation complication. Green’s second identity is invoked along with the Sommerfeld condition for acoustic scattering in chapter 3. However, both of these sources utilize a layer-potential rather than a direct BIE approach. This paper makes no assertion about these formulations, as the *source distribution* may compensate for selective conjugation, and requires separate consideration.

The expressed guidance for the direct method comes from a *circa* 1988 conversation with Frank Rizzo. At the time, Professor Rizzo believed the BIE was not “of a complex variable” as the physical coordinates were real-valued. The divergence theorem was essentially being applied twice – once to the real part of the field and once to the real coefficients of the imaginary component. This reasoning seemed plausible and the method was predicting the *magnitude* of elastic scattering amplitudes with excellent precision as compared to SOV.

In contrast, Physics Nobel laureate Roger Penrose in section 12.9 of his 2006 book [15] asserts that patches of surface (\mathcal{S}) can be equivalently mapped to the complex-plane. Thus a complex-valued 0-form (\mathfrak{E}) can be considered to be a complex-valued function over a complex-valued domain. The mathematics terminology is that the surface coordinates have been “complexified”. Penrose further asserts that the powerful Newlander–Nirenburg [16] theorem concerning smooth 2D-surface manifolds with *almost complex structure* implies that we can interchangeably use either an interpretation of the boundary surface integral being over \mathbb{R}^2 , or over \mathbb{C} . Therefore conclusions based on a viewpoint of our Helmholtz equation’s domain being defined by a single complex value (Z) should hold regardless that our original formulation was in terms of a pair of real-valued coordinates. To clarify, our radiation and/or scattering BVP boundary qualifies mathematically as having almost complex structure.

5.1.3 Integration of holomorphic functions

If implications of the Stokes–Cartan normal derivatives cannot be dismissed, then the effect of the surface and volume integrals should be considered. In a very non-rigorous, but at least condensed fashion, the author asserts that spatial integration of a *holomorphic* function also creates a conjugation, as compared to real-valued integrals of real and imaginary component treated separately. Consider how integration “undoes” differentiation in the Fundamental Theorem of Calculus. The surface integral of eqn (35) then implements two sequential conjugations with no net effect. The LHS volume integral is over a real-valued delta function and the holomorphic pressure field. The odd number of spatial integrations then reduces to the conjugate of the actual pressure field.



5.2 Boundary integral equation with new reasoning and classical calculus notation

Recall that the incoming and outgoing wave Fundamental Solutions are complex conjugates, and that both are initially present in the G of eqn (1). Regardless of whether spatial differentiation creates conjugation or not, the same pair of functions would remain. Using physics reasoning, rather than mathematics, this author asserts that the conjugation by GST happens first and then the Sommerfeld boundary condition eliminates Green's function (now) representing incoming waves. Strictly speaking the Fundamental Solutions are meromorphic functions with the exception at their singular point. In an over simplification Nakahara [10] indicates that if the pole occurs ON the boundary as it does with the BIE, then holomorphic function theorems still apply.

In contrast to the pair of Fundamental Solutions, there is a unique pressure field with a unique gradient, the conjugation invoked by GST makes actual changes as compared to the traditional BIE. To be clear, physically attainable boundary conditions to the Helmholtz operator result in fields that are holomorphic.

Standard Dolbeault operator notation ($\bar{\partial}$) is also used in real function calculus with a subscript to denote a directional derivative (∂_n). Even with the overbar being a standard indication of conjugation, the meaning is reversed in these two systems. Assuming many readers, like the author, are more adept with classical calculus notion – the notation trend of eqn (35) continues with explicit directional derivative and conjugation (†) symbols. For exterior domain acoustic radiation BVP, the new BIE is:

$$P^\dagger + 2 \oint \{ {}^\dagger G[\nabla_n(P)]^\dagger \} dS = 2 \oint \{ P \nabla_n ({}^\dagger G) \} dS. \quad (40)$$

5.3 Radiation benchmark problems revisited

Perhaps the least convincing aspect of this effort thus far is the amount of symmetry (or anti-symmetry) in the problems which can be done analytically. They are truly “special” cases, if not arguably somewhat degenerate. In the pulsing (monopole-like) sphere, the entire surface moves in synchronization. Without loss of generality, one could define the pressure field on the surface at time = 0 to be entirely real. Then the P^\dagger term is unaltered from P . The conjugation on the pressure gradient field in eqn (40) (as compared to the traditional BIE) then fully remedies the discrepancy with the SOV solution.

For the sphere with the dipole-like motion, the two sides of the sphere are 180° out of phase. Again, without loss of generality, the velocity (surface pressure gradient) could be assumed as only imaginary. Conjugation only interchanges the side of the sphere which are positive versus negative imaginary. In the low frequency limit, the pressure is 90 out of phase with the velocity (meaning only real). Then the P^\dagger term is again unchanged. The result of eqn (40) would be unchanged from the tradition BIE and remain a match with the SOV result.

6 DISCUSSION AND FUTURE WORK

The author remains sceptical of how even such a nuanced difference could have gone unnoticed or unquestioned for so long. In many situations, this difference is without practical significance. The primary issue considered is the merger of BEM with a non-conjugating method – which could be unreliable. Additionally, even if the conclusions herein are erroneous, the math involved was decades old when the BEM technology was being implemented, and there is little record of any consideration. Cheng and Cheng [12] cite the generalized Green's theorem for non-self-adjoint operators (attributed to Morse and Fechbach). While the Helmholtz operator remains self-adjoint, the Sommerfeld condition



creates a non-reversible time situation. There is an analogous equation structure if one considers the conjugate as the adjoint, as would be appropriate.

More low-frequency scattering benchmark cases need to be executed, including a “soft” sphere and most importantly, the two medium problem. Future upgrades to the traditional two-medium scattering BIE need to be formulated and confirmed via simple BEM code at moderate frequencies.

ACKNOWLEDGEMENTS

The author would like to thank the Center for NDE at Iowa State University for support in the early stages of this reported investigation; and fondly acknowledges the personal guidance on the boundary integral equation method from the late Frank J. Rizzo [17].

REFERENCES

- [1] Katz, V.J., The history of Stokes’ theorem. *Mathematics Magazine*, **52**(3), pp. 146–156, 1979. DOI: 10.1080/0025570X.1979.11976770.
- [2] Cartan, E., *Les Systèmes Différentiels Extérieurs et leurs Applications Géométriques*, Herman: Paris, 1945.
- [3] Schafbuch, P.J., Rizzo, F.J. & Thompson, R.B., Boundary element method solutions for elastic wave scattering in 3D. *International Journal for Numerical Methods in Engineering*, **36**, pp. 437–455, 1993.
- [4] Schafbuch, P.J., Thompson, R.B. & Rizzo, F.J., Application of the boundary element method to elastic wave scattering by irregular defects. *Journal of Nondestructive Evaluation*, **9**, pp. 113–127, 1991.
- [5] Kirkup, S., The boundary element method in acoustics: A survey. *Applied Sciences*, **9**(8), p. 1642, 2019. DOI: 10.3390/app9081642.
- [6] Pierce, A.D., *ACOUSTICS An Introduction to its Physical Principles and Applications*, McGraw-Hill, 1981.
- [7] Morse, P.M., *Vibration and Sound*, 2nd ed., McGraw-Hill, 1948.
- [8] Morse, P.M. & Ingard, K.U., *Theoretical Acoustics*, McGraw-Hill, 1968.
- [9] Fortney, J.P., *A Visual Introduction to Differential Forms and Calculus on Manifolds*, Birkhäuser, 2018. DOI: 10.1007/978-3-319-96992-3.
- [10] Nakahara, M., *Geometry, Topology and Physics*, 2nd ed., IOP Publishing, 2003.
- [11] Wirtinger, W., Zur formalen theorie der funktionen von mehr komplexen veränderlichen. *Mathematische Annalen*, **97**, pp. 357–375, 1927. DOI: 10.1007/BF01447872.
- [12] Cheng, A.H.D. & Cheng, D.T., Heritage and early history of the boundary element method. *Engineering Analysis with Boundary Elements*, **29**, pp. 268–302, 2005.
- [13] Burton, A.J. & Miller, G., The application of integral equation methods to the numerical solution of some exterior boundary-value problems. *Proceedings of the Royal Society of London A Mathematical and Physical Sciences*, **323**(1553), pp. 201–210, 1971.
- [14] Colton, D. & Kress, R., *Integral Equation Methods in Scattering Theory*, Wiley, 1983.
- [15] Penrose, R., *A Complete Guide to the Laws of the Universe*, BCA, pp. 243–246, 2004.
- [16] Newlander, A. & Nirenberg, L., Complex analytic coordinates in almost complex manifolds. *Annals of Mathematics*, **65**(3), pp. 391–404, 1957.
- [17] Fairweather, G., Martin, P.A. & Rudolphi, T.J., Frank Rizzo and boundary integral equations. *Engineering Analysis with Boundary Elements*, **124**, pp. 137–141, 2021.

